© 2022. Published by The Company of Biologists Ltd | Journal of Experimental Biology (2022) 225, jeb243672. doi:10.1242/jeb.243672

RESEARCH ARTICLE

Arapaima gigas maintains gas exchange separation in severe aquatic hypoxia but does not suffer branchial oxygen loss

Magnus L. Aaskov[1,*,‡], Rasmus J. Jensen[1,*], Peter Vilhelm Skov[2], Chris M. Wood[3], Tobias Wang[1], Hans Malte[1] and Mark Bayley[1]

ABSTRACT

One of the most air-reliant obligate air-breathing fish is the South American *Arapaima gigas*, with substantially reduced gills impeding gas diffusion, thought to be a result of recurring aquatic hypoxia in its habitat. In normoxic water, *A. gigas* is reported to satisfy 70–80% of its O_2 requirement from the air while excreting 60–90% of its CO_2 to the water. If this pattern of gas exchange were to continue in severely hypoxic water, O_2 loss at the gills would be expected. We hypothesized therefore that partitioning of CO_2 would shift to the air phase in severe aquatic hypoxia, eliminating the risk of branchial O_2 loss. By adapting a respirometer designed to measure aquatic $\dot{M}_{O_2}/\dot{M}_{CO_2}$, we were able to run intermittent closed respirometry on both water and air phase for both of these gasses as well as sample water for N-waste measurements (ammonia-N, urea-N) so as to calculate metabolic fuel utilization. In contrast to our prediction, we found that partitioning of CO_2 excretion changed little between normoxia and severe hypoxia (83% versus 77% aquatic excretion, respectively) and at the same time there was no evidence of branchial O_2 loss in hypoxia. This indicates that *A. gigas* can utilize distinct transfer pathways for O_2 and CO_2. Routine and standard $\dot{M}_{O_2}$, N-waste excretion and metabolic fuel utilization did not change with water oxygenation. Metabolism was fuelled mostly by protein oxidation (53%), while carbohydrates and lipids accounted for 27% and 20%, respectively.

KEY WORDS: Air-breathing fish, Anoxia, Fuel use, Gas exchange, Respirometry, Teleost

INTRODUCTION

It is broadly accepted that air breathing in fish has evolved in response to recurring hypoxia in the aquatic environment (Bayley et al., 2018). Air-breathing fish are categorized as obligate or facultative, depending on whether they rely on aerial respiration or use it as a supplementary strategy for O_2 uptake (Johansen, 1970). While there is varying dependence on aerial O_2 uptake, there is general agreement that CO_2 excretion occurs predominantly across the gills (Rahn and Howell, 1976; Singh, 1976; Brauner and Val, 1996; Graham, 1997c; Gonzalez et al., 2010; Brauner et al., 2019; Pelster et al., 2020). This represents an interesting problem, because the circulatory system of air-breathing teleosts has an undivided heart (Olson, 1994; Ishimatsu, 2012). Hence, it is conceivable that O_2-rich blood returning from the air-breathing organ (ABO) may lose O_2 to the water in hypoxia during passage through the gill basket (Smatresk and Cameron, 1982; Smatresk, 1990; Graham, 1997a; Graham and Wegner, 2010). Actual evidence for O_2 loss is limited to very few studies. Randall et al. (1981a) estimated the O_2 loss for the bowfin (*Amia calva*) to be 7% in hypoxia (14 mmHg) based on rather derived calculations and incomplete blood oxygen affinities across temperature, while a branchial O_2 loss of approximately 10% was found in the spotted gar (*Lepisosteus oculatus*) in hypoxia (12 mmHg) by direct measurement of O_2 content in blood before and after transit through the branchial basket (Smatresk and Cameron, 1982). Finally, differences in O_2 content between inspired and expired water were measured in the facultative air-breathing armoured catfish (*Hypostomus pyrineusi*) by Scott et al. (2017). Here, evidence for minor O_2 loss was found in only 4 of 11 animals in severe hypoxia (2 mmHg).

Furthermore, in several of the lungfishes (Johansen et al., 1968; Burggren and Johansen, 1986) and in the teleost snakehead fish *Channa argus* (Ishimatsu and Itazawa, 1983), separation of blood flow through the undivided heart has been documented. Such separation allows for the continued excretion of CO_2 from deoxygenated blood into the water while protecting the O_2-rich blood from the ABO from the risk of O_2 loss during branchial passage if a branchial shunt is present, such as a highly reduced gill arch or a trans-branchial vessel.

One of the most air-reliant obligate air-breathing fish is *Arapaima gigas* (Osteoglossiformes) (Brauner et al., 2004), which is native to tropical South America. *Arapaima gigas* starts life as a water breather (1–5 g) (Frommel et al., 2021) as is probably the case with almost all air-breathing fish (Bayley et al., 2020), but rapidly transitions to an air breather, which is accompanied by a radical re-modelling of the gills (Brauner et al., 2004). The inter-lamellar space fills with cell mass and ionocytes migrate to cover the now column-shaped filaments (Brauner et al., 2004). This greatly increases the blood–water diffusion distance and reduces the capacity for O_2 uptake (Brauner et al., 2004). The percentage aquatic O_2 uptake after this transition is reduced to 20–30% under normoxic conditions, with the remaining O_2 requirements being satisfied by aerial O_2 uptake (Randall et al., 1978; Brauner and Val, 1996; Gonzalez et al., 2010; Pelster et al., 2020). During progressive aquatic hypoxia, O_2 partitioning is further skewed towards the air phase where it will ultimately account for 100% of O_2 uptake (Stevens and Holeton, 1978). In normoxia, however, *A. gigas* continues to excrete 60–90% of its metabolically produced CO_2 to the water (Randall et al., 1978; Brauner and Val, 1996; Gonzalez et al., 2010; Pelster et al., 2020). Severe hypoxia or even anoxia frequently occurs in the tropical freshwater habitats of *A. gigas*

[1]Zoophysiology, Department of Biology, Aarhus University, 8000C Aarhus, Denmark. [2]Technical University of Denmark, DTU Aqua, Section for Aquaculture, DK-9850 Hirtshals, Denmark. [3]Department of Zoology, University of British Columbia, Vancouver, BC, Canada V6T 1Z4.
*Co-first authors.

‡Author for correspondence (magnus.aaskov@bio.au.dk)

M.L.A., 0000-0001-9458-2854; R.J.J., 0000-0003-0131-4522; P.V.S., 0000-0001-7900-4431; C.M.W., 0000-0002-9542-2219; T.W., 0000-0002-4350-3682; H.M., 0000-0003-3460-1819; M.B., 0000-0001-8052-2551

Received 19 October 2021; Accepted 2 February 2022

(Johansen et al., 1978; Richards et al., 2007). However, no studies have yet looked at the effect of such deep aquatic hypoxia on the partitioning of CO_2 excretion or for evidence of O_2 loss to the water.

The reduced gill surface area and increased blood–water distance in *A. gigas* seem also to impair gill diffusion of ammonia, manifesting in an elevated blood total ammonia concentration despite mass-specific ammonia production being lower in larger fish (Gonzalez et al., 2010; Pelster et al., 2020; Wood et al., 2020). Severe aquatic hypoxia has been shown to reduce branchial ventilation in many fish (Graham et al., 1978; Mattias et al., 1998; Oliveira et al., 2004; Perry et al., 2009; Belão et al., 2011, 2015; Thomsen et al., 2017; Mandic et al., 2020). Wood et al. (2020) found a substantial reduction in ammonia excretion during aquatic hypoxia (31 mmHg) in *A. gigas*, suggestive of reduced branchial ventilation and/or diffusive conductance in aquatic hypoxia. If this is the case, then a shift in the partitioning of CO_2 excretion towards the air phase in severe hypoxia would be expected, which in turn would reduce the risk of branchial O_2 loss in hypoxic water. Indeed, Bayley et al. (2020) argued that the astounding growth rates observed in air-breathing fish grown in deeply hypoxic aquaculture ponds – which is certainly the case for *A. gigas*, growing to 10–15 kg within a year (Ramírez et al., 2018) – do not fit well with significant O_2 loss in hypoxic water.

Measurements of excreted CO_2 in water are notoriously difficult, because of the equilibration of this gas with the bicarbonate and carbonate pools in water (Wang et al., 2021). However, Harter et al. (2017) recently showed that by passing respirometer water through an aggregate of gas-permeable plastic, flushed on the other side with a constant gas medium, it was possible to measure water expired CO_2 using a gas analyser. Here, we expanded this approach using commercially available medical grade artificial lungs in combination with previously developed two-phase intermittent closed respirometry (Lefevre et al., 2011, 2012, 2016) to allow for steady-state simultaneous measurements of O_2 and CO_2 exchange in water and air, and nitrogenous waste (total ammonia-N plus urea-N) excretion into the water phase. This allowed us to test the hypothesis that during severe hypoxia, *A. gigas* will take measures to reduce the risk of O_2 loss through the gill (e.g. reduced diffusive conductance, reduced ventilation, blood shunting to non-respiratory pathways), which will then also shift partitioning of CO_2 towards the ABO. To test this, we exposed the fish to a level of aquatic hypoxia significantly below the P_{50} of the blood, which for *A. gigas* at 28°C is 21 mmHg (Johansen et al., 1978). If, however, the gas exchange partitioning was not changed during hypoxia, we hypothesized a branchial O_2 loss. This was tested simultaneously with the first hypothesis as the water P_{O_2} levels were continuously logged. Furthermore, we hypothesized that metabolic rate would be increased in hypoxia, as increased surfacing is energetically costly (Lefevre et al., 2013). Lastly, in light of the observation of Wood et al. (2020) of reduced ammonia excretion during aquatic hypoxia, we hypothesized that this might be reflected in a shift in metabolic fuel utilization.

MATERIALS AND METHODS

Simultaneous bimodal gas-exchange measurements

This study was conducted using two-phase respirometry to measure the simultaneous bimodal gas exchange of *A. gigas*. Intermittent closed respirometry was used to measure O_2 uptake and CO_2 excretion in the water phase and flow respirometry was used for both O_2 uptake and CO_2 excretion in the air phase. Measurement of O_2 uptake in both phases and CO_2 excretion to the air phase occurred only in the closed periods of the intermittent closed respirometry, while CO_2 excretion to the water from the closed period was measured during the open period.

Animals

Respirometry measurements were performed on 7 pirarucu, *Arapaima gigas* (Schinz 1822) (1055–2025 g, mean of 1583 g), at Aarhus University. The animals were obtained from the Aquaculture Association of Caqueta (ACUICA, Florencia, Colombia), transferred to holding facilities at Aarhus University, and grown to experimental size at 29.5°C in large fibreglass composite tanks (1000 l) connected to a recirculating system supplied with soft water (pH 7.7, conductance ∼160 µS cm^{-1}) at 29.5°C. The fish were fed to satiation once daily (on weekdays) using catfish feed (Sigma 811R 6 mm, BioMar A/S, Denmark; protein 44%, lipid 16%, carbohydrate 20.5%). From 24 h prior to experimentation, fish were isolated in separate tanks within the same system and fasted. Fasting was continued throughout the experimental protocol. The experiment was performed in compliance with the Danish Law for Animal Experimentation.

Experimental protocol

Respirometry protocol

Aerial and water $\dot{M}_{O_2}$ and $\dot{M}_{CO_2}$ for seven *A. gigas* were measured in normoxic (P_{O_2} 134.5±5.52 mmHg, mean±s.d.) and severely hypoxic (1.10±3.12 mmHg) soft non-chlorinated water (conductance ∼150 µS cm^{-1}, pH ∼7) at 28°C and a normoxic and normocapnic air phase (20.95% O_2, 0.04% CO_2). The fish were randomly divided into groups starting either in normoxic (N=4) or in severely hypoxic (N=3) water and moved into the respirometer chamber 1–2 h before the first measurement. Measurements were initiated in the late afternoon, lasting 17.5 h per treatment until the following morning to minimize disturbance. Each measurement consisted of two measurement periods, one in each treatment (i.e. normoxia or severe hypoxia) separated by a non-measurement period (∼7 h) during the daytime, totalling ∼42 h. During this non-measurement period, water oxygenation level was the same as in the first measurement period. After the second measurement period, the fish was removed from the respirometer and bacterial gas exchange was recorded. A CO_2 calibration measurement was performed by injecting a known quantity of CO_2 into the chamber.

The air and water phases were not separated, so diffusion between the two phases was possible. However, water P_{O_2} remained constant during background $\dot{M}_{O_2}$ measurements in severe hypoxia, giving no indication of diffusion from the normoxic air phase to the hypoxic water phase. The respirometer consisted of a water-filled cylinder (30.1 l) with a small air-filled box (818 ml) added at one end where the fish could air breathe, and the setup is shown in Fig. 1. The water level of the system resulted in a small intrusion of water into the air-phase box and a net air-phase volume of 704 ml. The cylinder was sealed at both ends and a closed circulation loop through the ends maintained continuous water flow for aquatic O_2 and N-waste measurements. Oxygen was therefore sampled continuously during the closed period while N-waste was sampled at the beginning and end of each closed period by taking water aliquots of 5 ml. Finally, an open-loop system for flushing the cylinder with water from a header tank (212 l) was added at each end of the respirometer. The air space of the box on top was flushed with two tubes and the outflow was measured with aerial flow-respirometry that were sealed during water flush to avoid respirometer water volume changes, using electrically controlled valves. Because of the design

Journal of Experimental Biology (2022) 225, jeb243672. doi:10.1242/jeb.243672

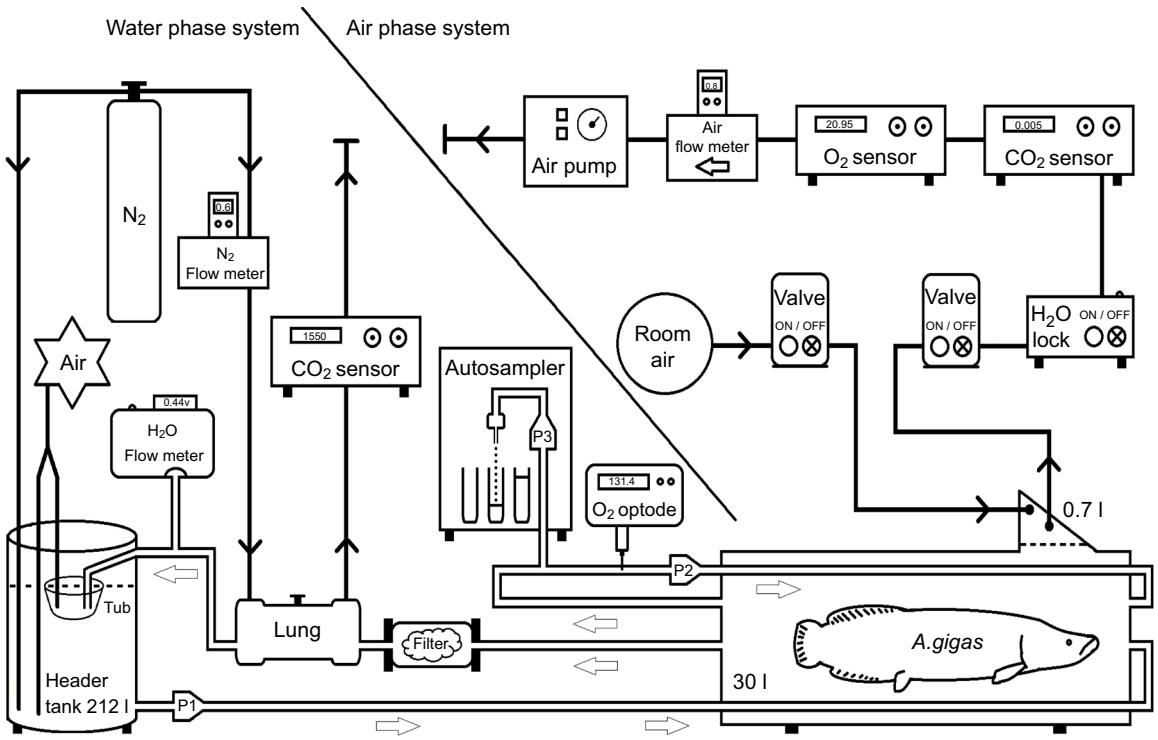

Fig. 1. Flow diagram showing the experimental setup to measure oxygen consumed and carbon dioxide (water and air phases) and nitrogen (water phase only) excreted by *Arapaima gigas*. P1 is the flush pump, P2 is the circulation pump and P3 is a peristaltic pump for the autosampler. Valves and pumps were controlled using an in-house system described in Lefevre et al. (2011). Outputs from the three gas analysers, from the flow meters and from the oxygen optode were digitized and stored using biopac and Acknowledge data sampling systems.

of the respirometer, it is possible that a small dead space was present near the water surface with reduced water circulation adding a resistance to O_2 diffusion into the water phase. If so, we judge this volume to have been very small relative to the 30 l respirometer volume.

Timing of measurements

Air phase

Gas exchange to the air phase was continuous. The air phase cycled through being open during the closed water respirometry period lasting 20 min and closed during water flushing lasting 15 min. Aerial gas exchange that occurred during the closed period was analysed upon opening of the air phase after each closed period.

Water phase

Water phase gas exchange was quantified for the closed periods and hence measured for 20 out of every 35 min.

Water phase O_2 uptake (intermittent closed respirometry)

O_2 consumption from the water ($\dot{M}_{O_2,water}$) was measured using intermittent closed respirometry as described previously (Lefevre et al., 2011, 2012, 2016). The sides of the tank were covered in black plastic to reduce visual stimuli. Hypoxia was achieved by bubbling a header tank (212 l), covered with plastic wrap, with N_2 while P_{O_2} was monitored with a Hamilton optode (Visifirm DO, Hamilton Company, Bonaduz, GR, Switzerland). The normoxic water was vigorously bubbled with air to maintain normoxia in the header tank, as water returning from the respirometer was O_2 depleted as a result of both fish respiration and O_2 removal in the artificial lung used for CO_2 measurements (see below). During the flush period, the respirometer water was renewed from the header tank maintained at either normoxia or severe hypoxia in an open-loop system returning to the header tank.

Logging of the $P_{O_2,water}$ measurements, opening and closing of the flush, and temperature management were automated by a software system (Respirometer 2.0) constructed at Zoophysiology, Aarhus University (Lefevre et al., 2011). The decline in $P_{O_2,water}$ was used to calculate O_2 consumption ($\dot{M}_{O_2}$) using Eqn 1:

$$\dot{M}_{O_2} = \frac{(\Delta P_{O_2}/\Delta t) \times \beta_{O_2} \times V_{sys}}{M_b}, \quad (1)$$

where ΔP_{O_2} is the absolute P_{O_2} decline in a closed period, Δt is the length of the closed period, β_{O_2} is the O_2 solubility, V_{sys} is the corrected volume of water in the respirometer (respirometer volume minus fish volume calculated from fish mass assuming a fish density of 1 kg l^{-1}) and M_b is the body mass. The bacterial O_2 consumption (background $\dot{M}_{O_2}$) was subtracted from the measurements.

To confirm the sensitivity of the system to detect O_2 loss by the fish, an analysis of detection limit was performed (see below) using the same level of hypoxia as in fish trials. Five different series were conducted with injections of O_2-saturated distilled water (0.5, 1.2, 2.5, 5 and 10 ml). Injections were made once per minute for 20 min. This corresponded to an O_2 appearance rate of 0.59, 1.48, 2.95, 5.90 and 11.66 µmol min^{-1}, respectively; for a typical 1.5 kg fish, in turn these rates corresponded to O_2 loss rates of 0.37, 0.93, 1.86, 3.73 and 7.37 µmol kg^{-1} min^{-1}.

Journal of Experimental Biology (2022) 225, jeb243672. doi:10.1242/jeb.243672

Water CO_2 excretion (intermittent closed respirometry)

The amount of CO_2 accumulated in the water during every closed period was measured by passing the water leaving the respirometer during the flush period through a modification of the system described by Harter et al. (2017). Hence, the outflow from the respirometer was flushed through an artificial lung (PrimO$_2$x oxygenator, Sorin Group Italy srl) to strip expired CO_2 from the respirometer into a carrier gas. The artificial lung has a multitude of parallel hollow fibre membranes where N_2 gas runs countercurrent to the water flow. This gives a very high area interface between the respirometry water and the N_2 carrier gas. CO_2 diffuses rapidly into the N_2 gas phase, where the concentration can be measured using a CO_2 analyser (Li-830 CO_2 gas analyser, LI-COR Biosciences, Lincoln, NE, USA), while water flow was logged (pressure transducer) to ensure it remained constant during a measurement loop. Here, the extraction was calculated against calibrations made by injecting known volumes of CO_2-saturated water into the respirometer while following the normal protocol timings. These calibration injections and background $\dot{M}_{O_2}$ measurements were performed after removal of the fish. Hence, these measurements were performed in both the normoxic and the severely hypoxic water for every replicate. The CO_2 injected was calculated using:

$$CO_{2,\text{injected}} = \alpha CO_2 \cdot P \cdot V, \quad (2)$$

where α is the CO_2 solubility in distilled water (µmol ml^{-1} mmHg^{-1}) (Dejours, 1981), P is the total gas pressure calculated by subtracting the water vapor pressure from the atmospheric pressure (760 mmHg) and V is the volume of the injected water.

The calibration factor was calculated using:

$$CO_{2,\text{calibration}} = \frac{CO_{2,\text{injected}}}{\int_{t_1}^{t_2} CO_{2,\text{measured}} - \int_{t_1}^{t_2} CO_{2,\text{bacteria}}}, \quad (3)$$

where $CO_{2,\text{injected}}$ is the total amount of CO_2 in the injected CO_2-saturated water, $\int_{t_1}^{t_2} CO_{2,\text{measured}}$ is the integral of the measured CO_2 between t_1 and t_2, and $\int_{t_1}^{t_2} CO_{2,\text{bacteria}}$ is the corresponding bacterial CO_2 production. Using this factor, the concentration can then be calculated:

$$CO_2 \text{ accumulated per period} = CO_{2,\text{calibration}} \times \left(\int_{t_1}^{t_2} CO_{2,\text{measured}} - \int_{t_1}^{t_2} CO_{2,\text{bacteria}} \right). \quad (4)$$

Eqn 4 assumes a linear relationship between P_{CO_2} in the water and measured CO_2. This assumption is supported by Harter et al. (2017) and our own measurements (Fig. S1).

Upon completion of a replicate, every part of the respirometer and tank was carefully cleaned using a biocidal agent (Virkon-S), and the gas analysers were calibrated before each run using 100% N_2 gas for the zero calibration, a mixture of 95% N_2 and 5% CO_2 gas for the CO_2 span (5%), and room air for the O_2 span (20.95%).

Air phase (intermittent flow respirometry)

O_2 consumption and CO_2 excretion with the normoxic and normocapnic air were measured using flow-through respirometry. Air flow was continuous except during water flush, where electronic valves sealed the air phase in the respirometer to prevent changes in water/air levels. Gas exchange occurring during the sealed period was recorded during the subsequent open air flow period. This sealing of the air phase during water flush resulted in P_{O_2} falling from the daily atmospheric level (ca. 155 mmHg) to a minimum of 117 mmHg and P_{CO_2} increasing from 0.03 to a maximum 21 mmHg. The air flow rate was measured using a mass flow meter (Sierra Instruments model 830D-L-1-V1) and water vapour was scrubbed from the air using anhydrous $CaCl_2$. $P_{O_2,\text{air}}$ and $P_{CO_2,\text{air}}$ were measured using a FC-10 Oxygen Analyzer and a CA-10 Carbon Dioxide Analyzer (Sable Systems Europe GmbH), respectively, and data logged with an MP100 biopac system (Biopac Systems Inc., Goleta, CA, USA) in AcqKnowledge (version 3.9.1, Biopac Systems Inc.).

Measurement of excreted total ammonia-N and urea-N

Water sampling

Respirometer water was sampled from the closed circulation loop at the beginning and end of each closed respirometry cycle using a time-programmable autosampler (Waters Fraction Collector III, Waters Corporation, Milford, MA, USA) connected to a peristaltic pump (Ole Dich, 115LMT, Hvidovre, Denmark) run by the respirometry program described above. There was already water in the autosampler tubing deadspace (4 ml) at the onset of each sampling. To avoid collecting mixed experimental water, we sampled experimental water in duplicate (2×5 ml) and discarded the first sample. The appropriate volume of the discarded sample (i.e. 5 ml) was determined by (1) filling the autosampler tubing deadspace with non-coloured water and then (2) sampling water coloured with greed food colorant (E161b and E133) until it fully replaced the non-coloured water.

During the unsupervised respirometry measurements, the autosampler tray was filled with ice in order to maintain samples at low temperature. All samples were capped and frozen at −20°C promptly after the final sampling for later analysis. The pH of the system ranged from 6.6 to 7.0, making diffusive NH_3 loss negligible.

Total ammonia-N and urea-N measurements

Total ammonia-N concentration was measured in water samples using the colorimetric method of Verdouw et al. (1978). Urea-N measurements (2 N per urea molecule) of water samples followed the colorimetric method of Rahmatullah and Boyde (1980).

Calculations

Nitrogen excretion

Ammonia and urea excretion rates were calculated from respective colorimetric assays to calculate the nitrogen quotient [NQ=(ammonia-N+urea-N)/$\dot{M}_{O_2}$], and the fish-specific respiratory quotient for protein (RQ_{protein}; the specific RQ value for protein varies from 0.83 to 0.97 depending on the N-excretory product) according to Lauff and Wood (1996).

To measure N-waste excretion during a 20 min closed period, each closed period was bracketed by chamber water sampling. However, it was not possible to measure N-waste elevation within single closed periods. This may have been due to limitations in the sensitivity of the N-waste assays, given the short duration of the closed period and the dilution of N-waste within the 30 l chamber. Instead, the excreted nitrogenous waste for the complete experimental period (17.5 h period per treatment) was calculated by measuring the rate of concentration increase in the whole system consisting of the combined volume of water in the respirometer, header tank and tubing (Fig. 1). Ammonia-N and urea-N excretion rates were then calculated by linear regression analysis (ammonia-N: r^2=0.58±0.06, range 0.29–0.88; urea-N: r^2=0.45±0.07, range 0.24–0.85) of the progressively increasing concentrations at the start

of each closed period, and these data are shown in Fig. S2:

$$\text{Ammonia-N or Urea-N excretion} = \frac{\text{Slope} \times V_{\text{sys}}}{M_{\text{b}}}, \quad (5)$$

where ammonia-N/urea-N excretion is in mol kg^{-1} min^{-1}, slope is in µmol l^{-1} min^{-1}, V_{sys} is the water volume in l of the entire system (chamber and header tank) and M_{b} is in kg. Hence, we calculated a single average N-waste excretion rate per fish per water treatment, for each of the two N-waste products.

Percentage fuel use

Fuel use (%) was calculated according to Lauff and Wood (1996). In short, the method uses measurements of respiratory exchange ratio (RER) and NQ to stoichiometrically calculate fractional metabolic fuel use contributions of the major aerobic fuels: carbohydrate, protein and lipid. RQ is assumed to be equal to RER under aerobic steady-state conditions, calculated by $\dot{M}_{\text{CO}_2}/\dot{M}_{\text{O}_2}$.

During the initial measurements, the fish were stressed as gas exchange was elevated and RER was generally well above 1, indicating either CO_2 generation from titration of bicarbonate produced by anaerobic metabolism or non-steady-state acid–base conditions in the plasma. RERs above 1 prevent calculation of fuel use (%) because the stoichiometric approach only works within the aerobic span of RER=0.7–1.0 (Kleiber, 1961). Therefore, all initial stressed measurements were excluded, and only the second measurement period was used for fuel use calculations. Fuel use calculations could not be performed on two fish because of incomplete datasets.

Data analysis

The mean±s.e.m. (N=3 normoxia, N=4 severe hypoxia) O_2 uptake and CO_2 excretion data from AcqKnowledge (version 3.9.1, Biopac Systems Inc.), were analysed in R. GraphPad Prism was used for the exponential decline analysis (GraphPad Software, San Diego, CA, USA). The total aerial O_2 taken up during one measurement period was calculated as the total integral of flow multiplied by the difference between the baseline and instantaneous oxygen fraction during that period. Hence, expressed mathematically:

$$\dot{M}_{\text{O}_2} = \int_0^T \dot{V}\,(F_{\text{baseline}} - F_{\text{O}_2}(t))\text{d}t = \dot{V}\int_0^T (F_{\text{baseline}} - F_{\text{O}_2}(t))\text{d}t, \quad (6)$$

where T is the time of the measurement period, F is the fractional concentration and $\dot{V}$ is the flow rate. Oxygen uptake rate was then calculated by dividing by measurement time. In a similar fashion, aerial $\dot{M}_{\text{CO}_2}$ for one measurement period was calculated as:

$$\dot{M}_{\text{CO}_2} = \dot{V}\int_0^T (F_{\text{CO}_2}(t) - F_{\text{baseline}})\text{d}t. \quad (7)$$

$\dot{M}_{\text{O}_2,\text{water}}$ was calculated with Eqn 1 and corrected for bacterial O_2 use by subtracting the measured background $\dot{M}_{\text{O}_2}$. $\dot{M}_{\text{CO}_2,\text{water}}$ was calculated as the increase in P_{CO_2} slope (total CO_2 integral−baseline CO_2) corrected for bacterial CO_2 production and multiplied by the calibration factor from Eqn 2. The changes in water phase baseline caused by both CO_2 accumulation during the experiment and removal either by the vigorous bubbling and/or the artificial lung were taken into account as each measurement had its own baseline. RER, total $\dot{M}_{\text{O}_2}$ and total $\dot{M}_{\text{CO}_2}$ were calculated for each loop (35 min period), and the difference in measuring periods between phases was accounted for by comparing the rates. Standard metabolic rate (SMR), based on $\dot{M}_{\text{O}_2}$ measurements, was calculated using the R script from Chabot et al. (2016) where the 10% quantile method was used (i.e. first group of deciles), and compared with a two-tailed Student's t-test. Loops were omitted if any O_2 or CO_2 value in any phase was missing, which could be caused by system failures or leaks. Linear mixed models in R with *lme4* (Bates et al., 2015) were used to account for repeated measures in time and fish. We used a random slope model with time and fish as random effects and water type (normoxia and hypoxia) as a fixed effect. The models estimated O_2 uptake and CO_2 excretion in air and water, and total values. They also estimated the fractional aerial $\dot{M}_{\text{O}_2}$, fractional aerial $\dot{M}_{\text{CO}_2}$, RER_{air}, $\text{RER}_{\text{water}}$, $\text{RER}_{\text{total}}$ and SMR. A semiparametric test to test for significance was made in R using *postHoc* (https://CRAN.R-project.org/package=postHoc) at a significance level of 0.05, where the P-values of the test for the pairwise comparisons were corrected by the single-step method described in Hothorn et al. (2015). The increasing concentrations used to calculate excretion of the N-waste (ammonia-N, urea-N) were analysed using a simple linear regression (GraphPad Prism 9). Differences in use of the three major aerobic metabolic fuels were analysed using a two-tailed t-test assuming unequal variances (Microsoft Excel).

RESULTS

General behaviour

Arapaima gigas appeared initially stressed after transfer to the respirometer. As the measurements started within 2 h of transfer, this stress was clearly evident in the initial $\dot{M}_{\text{O}_2}$ traces. The initial high O_2 uptake lasted longer in the hypoxic group than in the normoxic group. Additionally, there were occasional bouts of activity with continuous movement interspersed with more stationary behaviour with occasional surfacing glides to air breathe. Gill ventilation was observed in both normoxia and severe hypoxia and, while this was not measured, there were no apparent differences in gill ventilation between the normoxic and hypoxic water.

Effects of the initial stress

An exponential decline fitted to the average traces of fish started in normoxia (start normoxia) or severe hypoxia (start hypoxia) was made and compared to determine whether the decline followed the same trend in the two treatments. The two fitted curves were significantly different with a P-value of 0.0003 and could therefore not be fitted as one curve. The normoxic trendline showed a significantly faster return to baseline levels compared with the start of the hypoxic group. To exclude elevated stress values, an analysis of the exponential decline was made to obtain unbiased values of the plateau (Fig. 2). This test allowed the calculation of a time constant, τ, of 7.46 h for fish started in hypoxia and 5.84 h for fish started in normoxia: 3τ was used as a cut-off point to identify the end of stress, where 95% of the measurements did not deviate significantly from the plateau of the fitted exponential decline. This resulted in the removal of the first measurement period of fish started in severe hypoxia as their 3τ (3×7.46 h) exceeded the 17.5 h duration of the treatment. Hence, we used only the second measurement period for the statistical analysis of our hypotheses concerning CO_2 excretion and differences between normoxia and hypoxia (N=4 severe hypoxia and N=3 normoxia). For the O_2 loss measurement, all data of the 7 fish in severe hypoxia were used as stress is of interest here.

The initial stress period increased all parameters, especially in fish starting in severe hypoxia (Fig. 2). The large increases in CO_2

Journal of Experimental Biology (2022) 225, jeb243672. doi:10.1242/jeb.243672

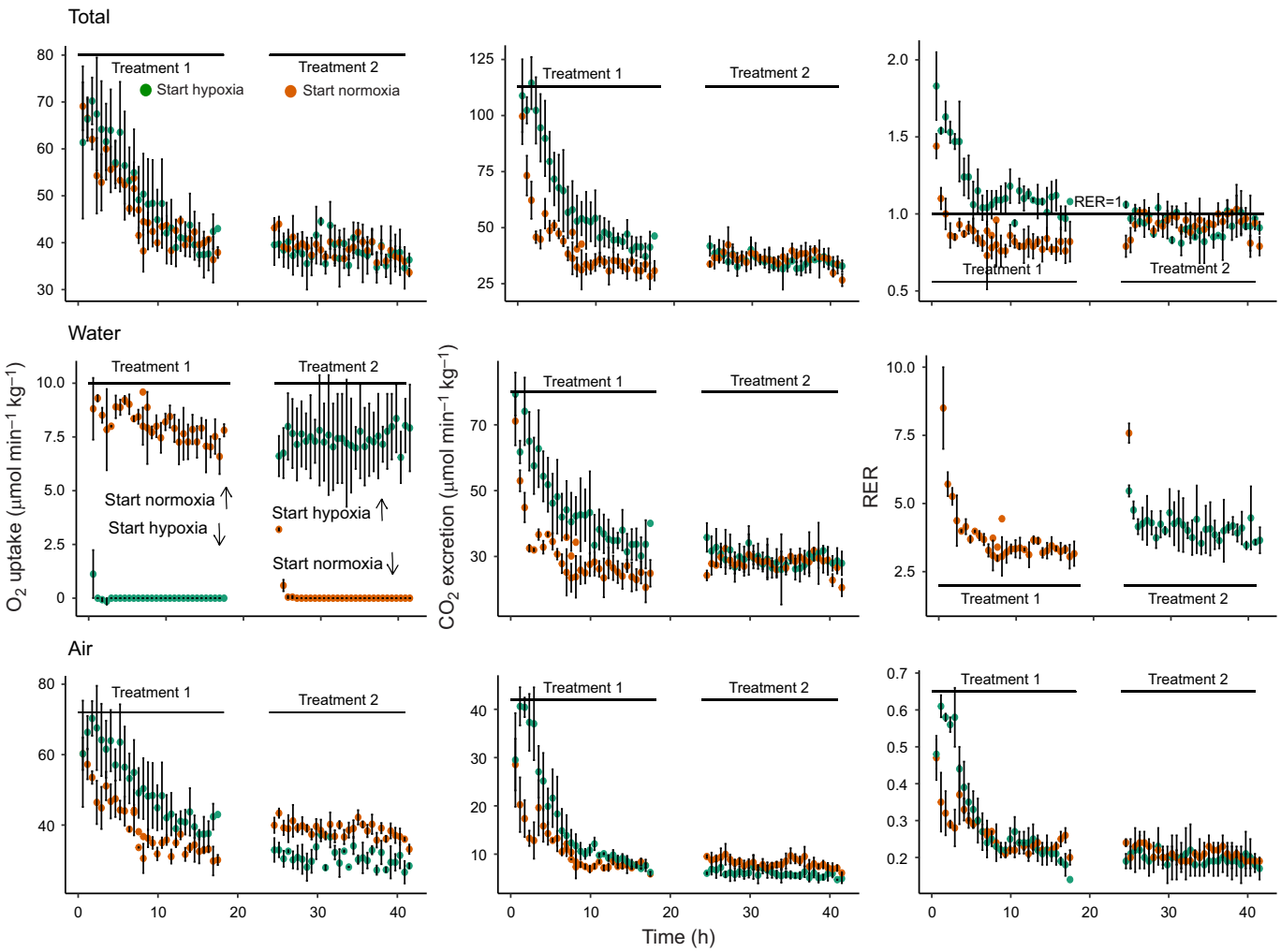

Fig. 2. Mean specific rates of O_2 uptake, CO_2 excretion and respiratory exchange ratio (RER). Data are for water and air combined (total) and separately. Green circles denote fish that started in hypoxic water (*N*=3) during the first treatment and orange circles denote fish that started in normoxic water (*N*=4) during the first treatment (total *N*=7). Water type (normoxia or hypoxia) was switched between treatments. Mean±s.e.m. mass was 1.583±0.292 kg.

excretion during stress were also evident in the aerial RERs and total RERs, which were initially much higher for the fish started in severe hypoxia. Once the stress period was passed, 80% of the O_2 was obtained from the air phase in normoxia against 100% in severe hypoxia (Table 1) whereas total O_2 uptake remained almost constant between the treatments, with estimates for SMR at 33 and 36 µmol min^{-1} kg^{-1} in normoxia and severe hypoxia, respectively.

Partitioning of gas exchange

Surprisingly, the aerial partitioning of CO_2 excretion changed little (though almost significant, P=0.051) when comparing fish in normoxia with those in severe hypoxia. The percentage aerial excretion was 17% in normoxia against 23% in severe hypoxia, which can be compared with the corresponding O_2 values, which changed from 80% to 100% (Table 1). This large increase in aerial O_2 uptake in hypoxic versus normoxic water was also accompanied by a significant increase in aerial CO_2 excretion, which rose from 5.7 to 8.7 µmol min^{-1} kg^{-1}. However, when viewing the total excretion of CO_2 in the two aquatic conditions, it is evident that water P_{O_2} of the two treatments had little impact and the water phase was the recipient of around 80% of the total metabolic excretion of CO_2 in both normoxia and severe hypoxia. The total O_2 uptake did not change significantly between treatments (P=0.42) and neither did total CO_2 excretion (P=0.34), which was reflected in a total RER of 0.94 and 0.96 for normoxia and severe hypoxia, respectively (P=0.59). Likewise, the SMR was not significantly different between fish in normoxia and those in severe hypoxia (P=0.26).

Lack of branchial O_2 leak

Diffusion of CO_2 from blood to water indicates a potential for O_2 loss by net diffusion in the severely hypoxic water where the blood/water P_{O_2} gradient would favour loss. However, no O_2 leak was detected in any of the fish (Fig. 3A), with the exception of two fish during the initial stressed period. In one of these (Fig. 3A, pink trace) there was an increase in water P_{O_2} in 9 of the initial 13 closed periods. The loss of oxygen in this fish corresponded to 0.5–1.36% of its total O_2 uptake in these closed respirometry loops. The second fish (Fig. 3A, orange trace) lost 0.59–0.82% of its total O_2 uptake in the corresponding loops. After around 200 min of severe hypoxia, only the small analog to digital conversion noise (which is unavoidable with the optode technology) raises the P_{O_2} above baseline and we concluded that O_2 loss from the fish was below our detection limit. The initial decrease in water P_{O_2} occurred because the initial flushes displaced the original normoxic water from the chamber to the severely hypoxic header tank, which then temporarily increased the header tank P_{O_2}.

Journal of Experimental Biology (2022) 225, jeb243672. doi:10.1242/jeb.243672

Table 1. Mass-specific O_2 uptake ($\dot{M}_{O_2}$) and CO_2 excretion ($\dot{M}_{CO_2}$) in *Arapaima gigas* in normoxia and severe hypoxia

	Normoxia	Severe hypoxia
$\dot{M}_{O_2,air}$ (μmol min^{-1} kg^{-1})	29.6±2.3	39.6±1.6*
$\dot{M}_{O_2,water}$ (μmol min^{-1} kg^{-1})	7.3±1.2	0.07±0.06*
$\dot{M}_{O_2,total}$ (μmol min^{-1} kg^{-1})	36.8±3.2	39.7±1.6
$\dot{M}_{CO_2,air}$ (μmol min^{-1} kg^{-1})	5.7±0.8	8.7±0.9*
$\dot{M}_{CO_2,water}$ (μmol min^{-1} kg^{-1})	28.8±2.8	29.4±2.0
$\dot{M}_{CO_2,total}$ (μmol min^{-1} kg^{-1})	34.5±3.0	38.1±2.9
Fraction aerial $\dot{M}_{O_2}$	0.80±0.02	1.0±0.001*
Fraction aerial $\dot{M}_{CO_2}$	0.17±0.03	0.23±0.01
RER air	0.20±0.03	0.22±0.01
RER water	4.1±0.41	
RER total	0.94±0.02	0.96±0.04
SMR (μmol min^{-1} kg^{-1})	32.8±2.5	36.2±1.4

Data (means±s.e.m.) were obtained during the second measurement period, when animals had become accustomed to the respirometer. The fractional aerial $\dot{M}_{O_2}$, fractional aerial $\dot{M}_{CO_2}$, respiratory exchange ratio (RER_{air}, RER_{water}, RER_{total}) and standard metabolic rate (SMR) are also shown. All values are estimates from a random slope model that takes the repeated measures into account. *N*=7 (normoxia *N*=3, severe hypoxia *N*=4), body mass 1.583±0.292 kg. *Significant difference between normoxia and hypoxia (*P*<0.05).

We performed an experiment to determine our detection limit for O_2 leakage from the fish (Fig. 3B) by injecting known volumes of O_2-saturated water into the respirometer without fish. This revealed that the lowest detectable level of O_2 addition to the water phase was between the lowest and second lowest O_2 injection amount. For an average fish mass in this experiment (1.583 kg), this detection limit would then translate to between 1.0% and 2.6% of their SMR (i.e. 0.36–0.94 μmol min^{-1} kg ^{1}). This means that O_2 loss if present in severe hypoxia would only represent a very small fraction of their O_2 uptake.

Total ammonia-N and urea-N excretion

Our estimate of ammonia-N excretion rate was slightly lower (4.80±0.64 μmol kg^{-1} min^{-1}) than found in previous studies on *A. gigas*, which have all been performed on animals with a lower mass than in the present study (Fig. 4B). Urea-N excretion rate was also slightly lower (0.69±0.25 μmol kg^{-1} min^{-1}) in comparison to previous values for juvenile *A. gigas* (<70 g) but similar to data found in animals of intermediate size (~0.65 kg) (Fig. 4A). Calculation of percentage urea-N [urea-N/([urea-N+ammonia-N)] revealed that urea excretion accounted for a small part of the total N-excretion (12.1±3.3%). One fish relied relatively heavily on urea excretion (25% urea-N) while the remaining fish relied much less on urea excretion (8.8±0.7% urea-N) (Fig. 4A).

$RQ_{protein}$ was high (0.96±0.004) given the low percentage urea-N. NQ was substantial (0.14±0.02) considering the fish's fasted state and none of the measurements exceeded the theoretical maximum NQ of 0.27 that indicates 100% protein utilization under aerobic and steady-state conditions. Aerobic metabolism was calculated to be fuelled predominantly by protein, which accounted for more than half of fuel burned (52.95±7.1%), which was about 2-fold higher than both carbohydrate (26.76±3.3%; *P*=0.015) and lipid (20.29±6.3%; *P*=0.009) (Fig. 5A). Carbohydrate and lipid utilization were similar and did not differ significantly (*P*=0.40). Fuel utilization resembled prior measurements in smaller *A. gigas* (0.625 kg), but carbohydrate use tended to be more prominent with slightly lower protein use (Fig. 5A). Effects of severe hypoxia were not analysed because of low replication. However, on the basis of our limited data, we could find no indication that severe hypoxia affected either N-waste excretion (Fig. 4) or fuel utilization (Fig. 5B).

DISCUSSION

Our primary goal was to investigate how partitioning of gas exchange in *A. gigas* changed when transitioning from aquatic normoxia to hypoxia and how metabolic rate in general was affected. We hypothesized that CO_2 partitioning would shift to the air phase and if not that we would detect an O_2 leak from the gills to the water. Surprisingly, our data show that aquatic CO_2 excretion remained practically unchanged in severe aquatic hypoxia compared with normoxia and that there was no evidence of branchial O_2 loss in hypoxic water except in two fish in the stressed period immediately after introduction into the respirometer.

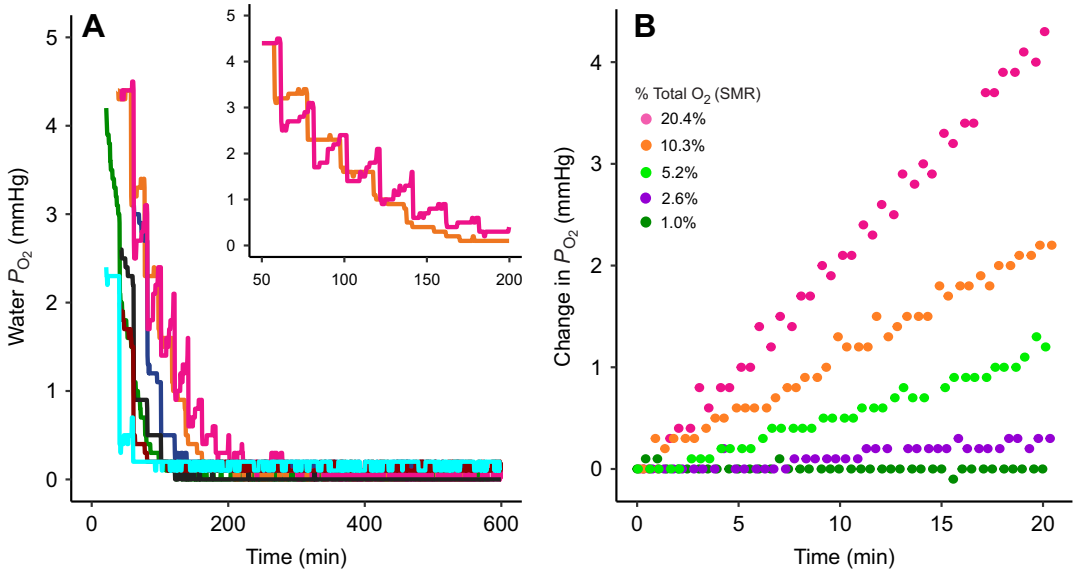

Fig. 3. Branchial O_2 leak and system detection limit. (A) A moving median of the water P_{O_2} during every closed loop of the severely hypoxic water measurements. Individual fish are shown by different colours (*N*=7). Inset shows traces of two fish where O_2 loss occurred. (B) Five different volumes of O_2-saturated water (0.5, 1.2, 2.5, 5 and 10 ml) were injected at a rate of one per minute for 20 min. The percentage total O_2 indicates the percentage of the hypoxia standard metabolic rate (SMR) that the injected volume is equal to.

Journal of Experimental Biology (2022) 225, jeb243672. doi:10.1242/jeb.243672

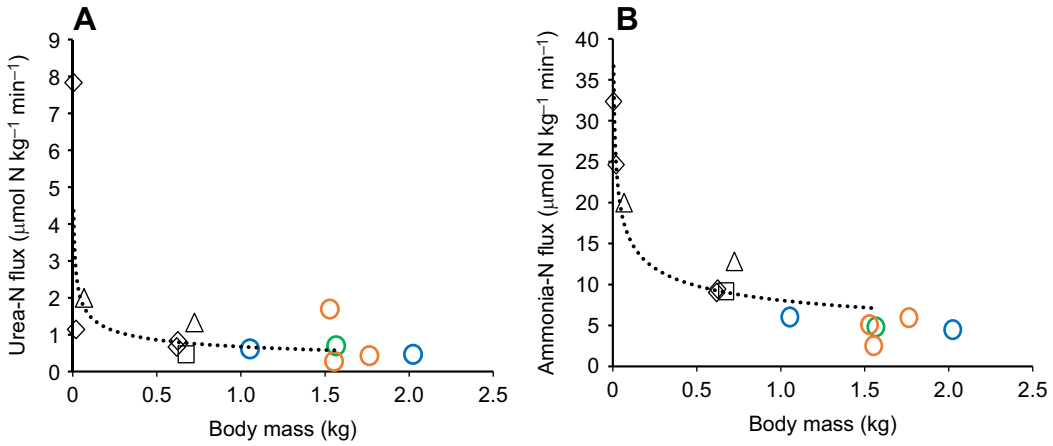

Fig. 4. Urea-N and ammonia-N flux according to fish body mass. Urea-N (A) and ammonia-N (B) flux are shown for individual fish (N=5) in the present study in water normoxia (blue) and severe hypoxia (red). Mean values for *A. gigas* fasted for 24 h (green circles; present study), 48 h (triangles; Gonzalez et al., 2010), 2–3 days (diamonds; Pelster et al., 2020) or 2–7 days (squares: Wood et al., 2020) are shown. s.e.m. (not shown in the figure for legibility: μmol N kg^{-1} min^{-1}): (A) mean 0.30, range 0.04–1.0; and (B) mean 1.2, range 0.83–2.5. The best-fit line for a power function is shown only for mean values for urea-N (y=0.673$x^{-0.352}$; r^2=0.78) and ammonia-N (y=8.1102$x^{-0.284}$; r^2=0.89).

Partitioning and O_2 loss

Although we saw a minor significant increase in aerial CO_2 excretion when *A. gigas* was exposed to severe aquatic hypoxia, the increase was modest in terms of the continued dominance of the water phase for CO_2 excretion. Overall, we failed to find evidence supporting our hypothesis that *A. gigas* changed its partitioning of CO_2 excretion when transitioning between normoxia and hypoxia. In aquatic hypoxia, 77% of the total produced CO_2 was excreted to the water phase compared with 83% in normoxia. The significant aerial elevation and small aquatic reduction are expected as the ABO is more strongly ventilated in hypoxia compared with normoxia. The aquatic CO_2 excretion in normoxic water in the present study is within the previously measured range of 63–89% (Randall et al., 1978; Brauner and Val, 1996; Gonzalez et al., 2010; Pelster et al., 2020). Despite the continued use of the water phase to excrete CO_2, the O_2 level (1.1 mmHg) of which was substantially below the blood P_{50} of *A. gigas* (21 mmHg; Johansen et al., 1978), we could find absolutely no evidence for any O_2 loss from fish that had become accustomed to the respirometer. Data from two stressed individuals immediately following introduction into the respirometer confirmed that O_2 can be lost as previously suggested (Randall et al., 1981a; Smatresk and Cameron, 1982; Scott et al., 2017). Here, the O_2 loss in this initial stressed state, though detectable, presented a minor fraction of total O_2 uptake at around 1.36% in the affected closed respirometer loops. Further, as these fish calmed with respirometer familiarity, this O_2 loss rapidly decreased to below the detection limit of the system. This is in line with Scott et al. (2017), who found branchial O_2 loss in 4 out of 11 instrumented armoured catfish, at a water P_{O_2} approaching the P_{O_2} (1.7 mmHg) at which loss of equilibrium occurred (Scott et al., 2017).

Increased diffusive resistance to O_2 seen in air-breathing fish gills compared with that in closely related water breathers is often seen as a strategy to reduce O_2 loss in hypoxia (Randall et al., 1981a,b; Graham, 1997b; Brauner et al., 2004; Phuong et al., 2017; Frommel et al., 2021). This includes both reductions in respiratory surface area and increases in epithelial thickness of the gills (Phuong et al., 2017, 2018). As *A. gigas* develops from the larval stage, its interlamellar spaces are filled with cells, resulting in a very small diffusive surface in animals of more than 5 g (Brauner et al., 2004; Frommel et al., 2021). Interestingly, these interlamellar cells do not appear to have been evaluated in terms of any potential plasticity

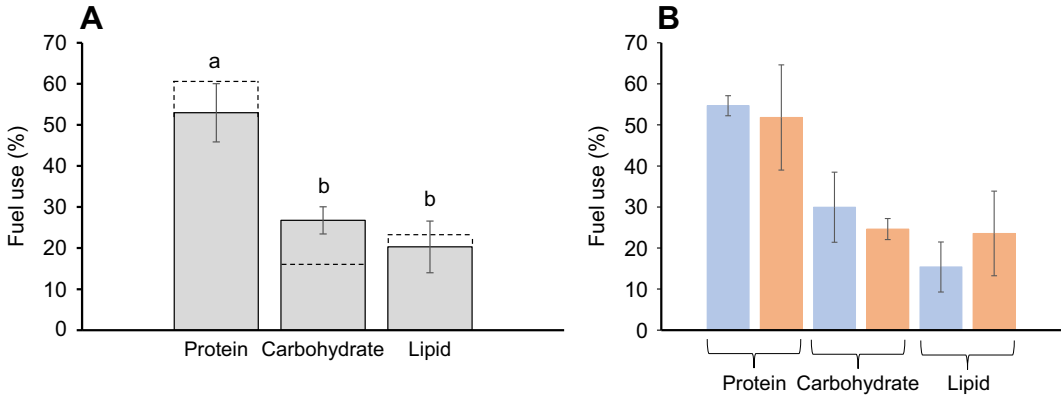

Fig. 5. Metabolic fuel use in *A. gigas*. (A) Protein, carbohydrate and lipid partitioning (N=5). (B) Fuel use in water normoxia (blue) and severe hypoxia (orange). Solid bars represent results from the present study and dashed lines indicate results from Pelster et al. (2020) for 625 g *A. gigas*; error bars are s.e.m. Significant differences are shown by different letters (α=0.05). Analysis: two-tailed t-test for difference between fuel use (A); analysis not possible for effect of normoxia (N=2) versus severe hypoxia (N=3) because of low replication (B).

with respect to water oxygen and animal metabolic requirements (e.g. Tzaneva et al., 2014; Phuong et al., 2018), which might be a promising line for future research.

Irrespective of any gill modifications that might reduce O_2 loss in hypoxia, our data show that most of the produced CO_2 is still excreted to the water, meaning that blood and water are not fully isolated. This continued CO_2 excretion to the water phase in deep hypoxia has been indirectly estimated in several other species of air-breathing fish based on very low aerial RER values (Hughes and Singh, 1970, 1971; Smatresk and Cameron, 1982; Graham, 1983; Yu and Woo, 1985). Even though the Krogh's diffusion constant for CO_2 is much larger than that for O_2, the excretion of CO_2 in the teleost gill is still limited by diffusion (Malte and Weber, 1985; Perry and Gilmour, 2002). The reduced diffusion conductance accompanying reduced gills decreases the ability of the gills to excrete CO_2, resulting in an elevated arterial P_{CO_2} (Brauner et al., 2004) to a new level where production is again matched by diffusive loss. In *A. gigas*, arterial P_{CO_2} has been measured to lie between 26 and 31 mmHg, which is approximately 10 times greater than for a typical water-breathing fish (2–3 mmHg) (Randall et al., 1978; Brauner et al., 2004). Hence, the reduced gills fit well with the measured arterial P_{CO_2}. This would also help explain the lack of concomitant O_2 loss in hypoxia. The high barrier for diffusion would especially limit O_2 compared with CO_2 as Krogh's diffusion constant (K) is 20–25 times higher for CO_2 (de Moraes et al., 2005). Whether these adaptations are sufficient to prevent O_2 loss to the degree documented here requires further investigation. Johansen et al. (1978) measured P_{O_2} in pre-branchial aortic blood in *A. gigas* as between 45 and 50 mmHg, leading these authors to predict a modest branchial O_2 loss.

An adaptation that might also facilitate this pattern of aquatic CO_2 excretion while completely preventing O_2 loss involves a trans-branchial shunt vessel, allowing blood to pass the gills without coming into contact with water. This would further require a continuous separation of blood flow from the ABO and systemic venous vessels rather than a convergence, through the heart and into either the arterial vessels leading to the ABO or the systemic circulation (Olson, 1994), because even with a gill shunt, there is still the problem of blood mixing during cardiac transit. This optimal organization of blood flow past the gills is known from several lungfish species but has also been functionally proven in the air-breathing teleost snakehead *Channa argus*. The lungfishes (*Lepidosiren*, *Neoceratodus*, *Protopterus*) have developed the most extensive modifications with various degrees of intracardiac septation and shunts approaching a parallel circulatory system not seen in other fish (Olson, 1994). The snakehead has extensive anatomical modifications inside the heart chambers and multiple ventral aortas that allow preferential diversion of oxygenated blood through degenerated gill arches (Ishimatsu and Itazawa, 1983). In another teleost, *Monopterus albus*, oxygenated and deoxygenated blood is shunted through branchial arteries that bypass the gills to the dorsal aorta (Iversen et al., 2013), although whether this represents an inefficiency in vascular layout or a functionally useful trait remains to be shown. *Arapaima gigas* does possess a possible shunt vessel given it has a vastly reduced 5th gill arch, which is devoid of lamellae; but again, any role this might play in avoiding O_2 loss remains an interesting avenue for future research.

The arrangement we therefore envisage that best fits our data is as follows. The CO_2-rich and O_2-poor blood of the venous return passes through the heart without fully mixing with the oxygenated but low-CO_2 blood from the ABO. This venous blood then loses CO_2 during branchial passage. In hypoxia, this can then occur with minimal oxygen loss because it is already de-oxygenated. After branchial passage, this blood is then transferred to the ABO where it is oxygenated, and where there is some minor further CO_2 excretion. In normoxia, this branchial passage will also allow for some oxygen uptake, but the greatly reduced *A. gigas* gills only then allow for 20% of the total oxygen uptake. The subsequent passage to the ABO allows for the remaining 80% and again here CO_2 is lost at the gills and therefore is not seen in expired gas from the ABO to any great degree. Conversely, the O_2-rich and decarbonated blood leaving the ABO passes the heart without effective mixing with the venous flow and must therefore then be shunted past the branchial basket for distribution to the body.

This proposed arrangement would seem utterly implausible were it not for the fact that such trans-cardiac flow separations and branchial shunts are already known in lungfish and the snakehead *C. argus* (Olson, 1994). Lungfish separate blood flow through the heart (Johansen et al., 1968; Graham, 1997d) with the aid of both ventrolateral and spiral folds in the bulbus arteriosus lumen (Scadeng et al., 2020) as well as incomplete septa and valves within the heart (Johansen et al., 1968; Graham, 1997d). *Channa argus* achieves intra-cardiac flow separation through a simpler arrangement with many ventricular pockets and longitudinal ridges in the bulbus (Ishimatsu and Itazawa, 1983), which resemble the amphibian heart. Based on the high O_2 saturation and P_{O_2} in the ventral aorta (80–90% and 45–50 mmHg, respectively; Johansen et al., 1978), Greenwood and Liem (1984) argued that mixing of systemic venous blood with the return from the ABO was probably small in *A. gigas*. The heart of *A. gigas* also possesses interesting morphological features that may promote flow separation within the heart, including a completely trabeculated ventricle (Buzete Gardinal et al., 2019; Scadeng et al., 2020) and a bulbus arteriosus lumen filled with elaborate tissue folds (Scadeng et al., 2020). The exact balance between diffusion and perfusion of oxygen and CO_2 and the degree of necessary flow separation is rather complex and a current focus through modelling in our laboratories. Nevertheless, the actual solution to produce the phenomenon measured in the present study would clearly not require complete separation of the ABO and systemic venous return. Thus, in addition to theoretical models of gas exchange, it would be of interest to measure blood gases at several sites and to describe the anatomy of the inflow to the heart as well as the arterial supply to the branchial basket.

Metabolic rate measurements

We were able to fully automate the intermittent respirometry system allowing for unsupervised measurements of O_2 and CO_2 in both phases and sampling of chamber water for excreted nitrogen in the water. The long duration (17 h per treatment) of multiple uninterrupted measurements allowed for calculation of partitioning of gas exchange and fuel utilization.

As measurements were started 1–2 h after the fish had been moved to the respirometer, the overall shapes of the O_2 and CO_2 traces (Fig. 2) follow the expected trend of an exponential decline until plateau (Keys, 1930), usually seen with an initial phase with stress and the likely involvement of anaerobic metabolism. Handling has been shown to increase the O_2 consumption of juvenile salmon by 39–98%, while also increasing whole-body lactate concentration by 500% compared with controls (Davis and Schreck, 1997). In the present study, the initial $\dot{M}_{O_2,total}$ was elevated by 89% above the unstressed plateau (Fig. 2). The elevation in CO_2 excretion was even more pronounced and disappeared more slowly, particularly in fish started in hypoxia. A high cytosolic ATP

Journal of Experimental Biology (2022) 225, jeb243672. doi:10.1242/jeb.243672

Table 2. Metabolic rate and gas exchange partitioning data for *A. gigas* from the literature

	Reference										
	1	2	3	2	1	4	Present	2	Present	5	6
Method	Closed resp.	Closed resp.	–	Closed resp.	Closed resp.	Closed resp.	Int. closed	Closed resp.	Int. closed	Closed resp.	ABO gas samples
M_b (kg)	0.0047	0.0675	1	0.0675	0.687	2–3	1–2	0.724	1–2	1.7	2
Temperature (°C)	27–29	28	28	28	27–29	27–29	28	28	28		–
RER	0.72 total	–	0.14 aerial	–	0.91 total	–	0.96 total	–	0.94 total		0.38 bladder
Water CO_2 excretion	97%	84.8%	–	85.7%	88%	–	78%	89%	83%	85.3%	63%
Water O_2 uptake	37%	21.9%	–	23.9%	25%	25%	0%	30.1%	20%	21.9%	22%
Total $\dot{M}_{CO_2}$ excretion (μmol kg^{-1} min^{-1})	133.0	–	–	–	61.2	–	38.12**	–	34.49	–	–
Total $\dot{M}_{O_2}$ uptake (μmol kg^{-1} min^{-1})	186.2	131.2*	117.4**	103.1	61.2	53.6	39.67**	38.0	36.82	–	–

The table shows the method used (closed respirometry, intermittent closed respirometry and gas samples from the air-breathing organ, ABO), fish body mass (M_b), temperature, RER, CO_2 and O_2 partitioning, and $\dot{M}_{CO_2}$ and $\dot{M}_{O_2}$ (*purposely disturbed; **aquatic hypoxic conditions, resting metabolic rate used). References: [1]Pelster et al. (2020); [2]Gonzalez et al. (2010); [3]Johansen et al. (1978); [4]Stevens and Holeton (1978); [5]Brauner and Val (1996); [6]Randall et al. (1978).

breakdown would have resulted in reduced pH titrating HCO_3^- and elevating blood P_{CO_2} and hence CO_2 excretion (Robergs et al., 2004), while a high production of lactate would aid in the elevated post-exercise gas exchange requirement, as it is known in teleosts that the lactate ion has a strong stimulatory effect on ventilation (Thomsen et al., 2017; Thomsen et al., 2019). This non-metabolically produced CO_2 can then elevate RER above 1, which was clearly evident in the entire first measurement period (Fig. 2). Robust evidence for elevated post-stress RER of this magnitude does not exist in the fish literature but is well documented in terrestrial tetrapods. For example, RER can reach 1.4 after exercise in cane toads (*Rhinella marinus*) and may reach 2.5 in the American alligator (*Alligator mississippiensis*) (Andersen and Wang, 2003; Hartzler et al., 2006).

In contrast to our initial hypothesis, we found no elevation of total $\dot{M}_{O_2}$ or SMR in severe hypoxia compared with normoxia. The cost of surfacing was probably very low in this study as surfacing behaviour is similar in normoxia and hypoxia, and the distance to the water surface is small.

O_2 uptake from water accounted for 20% of total O_2 uptake in normoxia. This O_2 partitioning agrees well with other studies of similarly sized *A. gigas* that have estimated this fraction to range from 21.9% to 25% (Table 2). Aerial O_2 uptake increased to 100% in severe hypoxia, which is expected based on earlier observations (Stevens and Holeton, 1978) and given that, in our experiment, ventral aortic blood P_{O_2} was almost certainly well in excess of water P_{O_2} in the water hypoxia treatment. The mass-specific rates of O_2 uptake and CO_2 excretion found in this study were considerably lower than most previous findings in *A. gigas* (Table 2), probably because of differences in fish mass between studies, and the use of intermittent flow respirometry instead of closed respirometry. Using the allometric scaling coefficient for $\dot{M}_{O_2}$ (0.776) and $\dot{M}_{CO_2}$ (0.843) from Pelster et al. (2020) to upscale their 0.687 kg fish to the mean mass (1.583 kg) of the current fish, our $\dot{M}_{O_2}$ and $\dot{M}_{CO_2}$ values are still, respectively, 27% and 32% lower than theirs. Both studies use a temperature of ∼28°C and the difference must therefore be attributed to the different methodology.

The SMR found in this study is at the low end of the range measured in other air-breathing fish species at similar temperature (Lefevre et al., 2014). The SMR of *A. gigas* is even low when considering its carnivorous sit and wait predation lifestyle and comparing it with that of other tropical, benthic and sluggish fish (Lefevre et al., 2014). *Arapaima gigas* shows a near-endothermic growth rate of around 10–15 kg year^{-1} (de Oliveira et al., 2012), and it may well be that its low householding costs contribute to this.

Nitrogen waste excretion

Table 3 shows N-waste and fuel use parameters in *A. gigas* from the literature. Using the scaling coefficient from Pelster et al. (2020) for ammonia-N (0.724), urea-N (0.730) and total-N (0.718) to upscale their data for 0.687 kg *A. gigas* to 1.583 kg, our ammonia-N and total-N measurements, respectively, are 56% and 47% lower than expected while our urea-N is 7.3% higher. We judge these differences to be minor when considering the lower overall metabolic rate in this study as discussed above. Contrary to our expectations based on a previous report where *A. gigas* were

Table 3. N-waste excretion and fuel use in *A. gigas* from the literature

Ammonia-N (μmol min^{-1} kg^{-1})	Urea-N (μmol min^{-1} kg^{-1})	Urea-N (%)	NQ	Fuel (%)			Fast (days)	Temp. (°C)	M_b (kg)	Reference
				P	C	L				
32.4	7.83	19.5	0.22	81.5	0.0	18.5	2–3	27–29	0.005	Pelster et al. (2020)
24.6	1.14	4.4	–	–	–	–	2–3	27–29	0.02	Pelster et al. (2020)
20	2	7.7	0.21	79.1	–	–	2	28	0.0675	Gonzalez et al. (2010)
9.0	0.67	6.9	–	–	–	–	2–3	27–29	0.619	Pelster et al. (2020)
9.4	0.83	8.1	0.16	60.6	16.2	23.2	2–3	27–29	0.625	Pelster et al. (2020)
9.2	0.47	4.8	–	–	–	–	2–7	27–29	0.675	Wood et al. (2020)
12.8	1.33	7.4	0.37	>100	–	–	2	28	0.724	Gonzalez et al. (2010)
4.8	0.69	12.1	0.14	53.0	26.8	20.3	1	28	1.57	Present study

NQ, nitrogen quotient; P, protein; C, carbohydrate; L, lipid.

exposed to moderate hypoxia (Wood et al., 2020), severe water hypoxia did not seem to affect total ammonia-N excretion rates (Fig. 4). Total urea-N excretion rates were also unaffected, which is in agreement with Wood et al. (2020). Similarly, no trends in metabolic fuel use were apparent as a result of changes in water oxygenation (Fig. 5B), in contrast to our initial hypothesis. As in previous studies on fasted individuals of this species, we found that nitrogen was predominantly excreted as ammonia-N. Urea-N contributed 12.1±3.3% to the total N-excretion, which is slightly more than in the previously studied smaller fish (0.02–0.7 kg) where the urea-N contribution ranged from 5% to 10%. However, this discrepancy was in large part due to a single individual with 25% urea-N, while the remaining fish averaged just 8.8±0.7% in line with previous data (Gonzalez et al., 2010; Pelster et al., 2020; Wood et al., 2020).

NQ, which correlates with the fractional contribution of protein oxidation to the entire aerobic metabolism, was 0.14, and well below the theoretical maximum of 0.27 (Lauff and Wood, 1996). Our values are close to earlier measurements on *A. gigas* that ranged from 0.16 to 0.22 (Gonzalez et al., 2010; Pelster et al., 2020). Additionally, an NQ of 0.16 and protein use of 58% can be estimated for Wood et al. (2020) if assuming an $\dot{M}_{O_2}$ as measured by Pelster et al. (2020) for *A. gigas* of similar age (3–4 months) and size (675 and 625 g, respectively), which is similar to the present study. For much smaller *A. gigas* (5 and 67 g), protein use was found to be higher at ∼80% (Gonzalez et al., 2010; Pelster et al., 2020).

This great reliance on protein to fuel aerobic metabolism in *A. gigas* during fasting is in line with values in satiation-fed juvenile rainbow trout (*Oncorhynchus mykiss*) (50–70% protein use) that rely much less on protein burning during fasting (15% protein use) (Alsop and Wood, 1997). However, this high protein use may simply reflect the diet. How fuel use changes after feeding has been studied in zebra fish (*Danio rerio*), where there was a post-prandial increased reliance on protein oxidation as digestion proceeded. The 48 h fasted zebra fish had a 26.8% protein fuel use while in fed zebra fish, protein fuel use progressively increased to about 52% at 7–10 h after feeding (Ferreira et al., 2019). This post-prandial increased reliance on protein burning is expected as dietary free amino acids in excess of anabolic needs must be oxidized if not converted to other fuel classes (Cowey, 1980). Therefore, it is possible that the high protein fuel use measured in *A. gigas* is a consequence of measurements being made relatively soon after feeding (≤3 days) (Gonzalez et al., 2010; Pelster et al., 2020). The nutritional status of our 24 h fasted *A. gigas* was probably still affected by the last meal consumed, as we sometimes detected tiny amounts of faeces in the respirometer. Feeding experiments followed by longer fasting periods might elucidate whether the current literature reflects truly fasted fish oxidizing their energy stores.

Conclusion

In conclusion, our two-phase intermittent closed respirometry in combination with nitrogenous waste sampling allows for complete respirometric measurements to assess fuel utilization by the stoichiometric approach. This method allowing multiple uninterrupted measurements makes it possible to separate activity from basal metabolism. We found no functional change in the partitioning of CO_2 excretion between water and air during exposure to severe hypoxia, with the aquatic fraction remaining around 80%. There was a small but significant increase in aerial CO_2 excretion, which we believe results from the increased ventilation of the ABO in aquatic hypoxia, where 100% of the O_2 uptake is aerial. We did not detect any sign of branchial O_2 loss in severe hypoxia, except in two very stressed fish soon after the fish was introduced to the respirometer. We argue that the absence of oxygen loss is probably a result of both the reduced gills in this species, which would especially limit O_2 compared with CO_2 as Krogh's diffusion constant (K) is 20–25 times higher for CO_2 (de Moraes et al., 2005), and also an unknown anatomical arrangement promoting diversion of oxygenated blood away from the branchial respiratory surfaces. We found no effect of hypoxia on total ammonia-N and urea-N excretion. This is in accordance with the finding of no change in aquatic CO_2 excretion. We found that metabolic fuel use was dominated by protein (53%), with near-equal contributions from carbohydrate (27%) and lipid (20%).

Acknowledgements

We thank Heidi M. Jensen, Erik Paima and Claus Wandborg for assistance in the animal facility. We also thank John S. Jensen and Jesper R. Voetmann for building our respirometer chambers and Kristian Beedholm for hardware construction and programming. Finally, we thank Per G. Henriksen for laboratory guidance.

Competing interests

The authors declare no competing or financial interests.

Author contributions

Conceptualization: C.M.W., H.M., M.B.; Methodology: M.L.A., R.J.J., H.M., M.B.; Validation: M.L.A., R.J.J., H.M., M.B.; Formal analysis: M.L.A., R.J.J., H.M.; Investigation: M.L.A., R.J.J.; Resources: P.V.S., M.B.; Data curation: M.L.A., R.J.J.; Writing - original draft: M.L.A., R.J.J., M.B.; Writing - review & editing: P.V.S., C.M.W., T.W., H.M., M.B.; Supervision: H.M., M.B.; Funding acquisition: M.B.

Funding

This research was funded by the Danish Council for Independent Research|Natural Sciences (Natur og Univers, Det Frie Forskningsråd); grant no. 0135-00256B.

Data availability

Data are available from Zenodo: https://zenodo.org/record/6322428#.Yh876rrMI2w.

References

Alsop, D. and Wood, C. (1997). The interactive effects of feeding and exercise on oxygen consumption, swimming performance and protein usage in juvenile rainbow trout (Oncorhynchus mykiss). *J. Exp. Biol.* **200**, 2337-2346. doi:10.1242/jeb.200.17.2337

Andersen, J. B. and Wang, T. (2003). Cardiorespiratory effects of forced activity and digestion in toads. *Physiol. Biochem. Zool.* **76**, 459-470. doi:10.1086/375439

Bates, D., Mächler, M., Bolker, B. and Walker, S. (2015). Fitting linear mixed-effects models using lme4. *J. Stat. Softw.* **67**, 48. doi:10.18637/jss.v067.i01

Bayley, M., Damsgaard, C., Thomsen, M., Malte, H. and Wang, T. (2018). Learning to air-breathe: the first steps. *Physiology* **34**, 14-29. doi:10.1152/physiol.00028.2018

Bayley, M., Damsgaard, C., Cong, N., Phuong, N. and Do, H. (2020). Aquaculture of air-breathing fishes. In *Fish Physiology*, Vol. 38, pp. 315-353. Academic Press.

Belão, T. C., Leite, C. A. C., Florindo, L. H., Kalinin, A. L. and Rantin, F. T. (2011). Cardiorespiratory responses to hypoxia in the African catfish, Clarias gariepinus (Burchell 1822), an air-breathing fish. *J. Comp. Physiol. B* **181**, 905. doi:10.1007/s00360-011-0577-z

Belão, T. C., Zeraik, V. M., Florindo, L. H., Kalinin, A. L., Leite, C. A. C. and Rantin, F. T. (2015). Control of cardiorespiratory function in response to hypoxia in an air-breathing fish, the African sharptooth catfish, Clarias gariepinus. *Comp. Biochem. Physiol. A Mol. Integr. Physiol.* **187**, 130-140. doi:10.1016/j.cbpa.2015.05.010

Brauner, C. J. and Val, A. L. (1996). The interaction between O2 and CO2 exchange in the obligate air breather, Arapaima gigas, and the facultative air breather, Lipossarcus pardalis. In *Physiology and Biochemistry of the Fishes of the Amazon* (ed. A. L. Val, V. M. F. Almeida-Val and D. J. Randall), pp. 101. Manaus, Brazil: INPA.

Brauner, C. J., Matey, V., Wilson, J. M., Bernier, N. J. and Val, A. L. (2004). Transition in organ function during the evolution of air-breathing; insights from Arapaima gigas, an obligate air-breathing teleost from the Amazon. *J. Exp. Biol.* **207**, 1433. doi:10.1242/jeb.00887

Brauner, C. J., Shartau, R. B., Damsgaard, C., Esbaugh, A. J., Wilson, R. W. and Grosell, M. (2019). 3 - Acid-base physiology and CO2 homeostasis: Regulation and compensation in response to elevated environmental CO2. In *Fish Physiology*, Vol. 37. (eds. M. Grosell, P. L. Munday, A. P. Farrell and C. J. Brauner), pp. 69-132: Academic Press.

Burggren, W. W. and Johansen, K. (1986). Circulation and respiration in lungfishes (dipnoi). *J. Morphol.* **190**, 217-236. doi:10.1002/jmor.1051900415

Buzete Gardinal, M. V., Rocha Ruiz, T. F., Estevan Moron, S., Oba Yoshioka, E. T., Uribe Gonçalves, L., Franceschini Vicentini, I. B. and Vicentini, C. A. (2019). Heart structure in the Amazonian teleost Arapaima gigas (Osteoglossiformes, Arapaimidae). *J. Anat.* **234**, 327-337. doi:10.1111/joa.12919

Chabot, D., Steffensen, J. F. and Farrell, A. P. (2016). The determination of standard metabolic rate in fishes. *J. Fish Biol.* **88**, 81-121. doi:10.1111/jfb.12845

Cowey, C. (1980). Protein metabolism in fish. In *Protein Deposition in Animals*, (ed. D. B. Lindsay), pp. 271-288. Butterworths London.

Davis, L. E. and Schreck, C. B. (1997). The energetic response to handling stress in Juvenile Coho Salmon. *Trans. Am. Fish. Soc.* **126**, 248-258. doi:10.1577/1548-8659(1997)126<0248:TERTHS>2.3.CO;2

de Moraes, M. F. P. G. d., Höller, S., da Costa, O. T. F., Glass, M. L., Fernandes, M. N. and Perry, S. F. (2005). Morphometric comparison of the respiratory organs in the south american lungfish Lepidosiren paradoxa (Dipnoi). *Physiol. Biochem. Zool.* **78**, 546-559. doi:10.1086/430686

de Oliveira, E. G., Pinheiro, A. B., de Oliveira, V. Q., da Silva, A. R. M., de Moraes, M. G., Rocha, R. C. B., de Sousa, R. R. and Costa, F. H. F. (2012). Effects of stocking density on the performance of juvenile pirarucu (Arapaima gigas) in cages. *Aquaculture* **370-371**, 96-101. doi:10.1016/j.aquaculture.2012.09.027

Dejours, P. (1981). *Principles of Comparative Respiratory Physiology*. Amsterdam: North-Holland Publishing Company.

Ferreira, M. S., Wood, C. M., Harter, T. S., Dal Pont, G., Val, A. L. and Matthews, P. G. D. (2019). Metabolic fuel use after feeding in the zebrafish (Danio rerio): a respirometric analysis. *J. Exp. Biol.* **222**, jeb194217. doi:10.1242/jeb.194217

Frommel, A. Y., Kwan, G. T., Prime, K. J., Tresguerres, M., Lauridsen, H., Val, A. L., Gonçalves, L. U. and Brauner, C. J. (2021). Changes in gill and air-breathing organ characteristics during the transition from water- to air-breathing in juvenile Arapaima gigas. *J. Exp. Zool. A Ecol. Integr. Physiol.* **335**, 801-813, Epub ahead of print. doi:10.1002/jez.2456

Gonzalez, R. J., Brauner, C. J., Wang, Y. X., Richards, J. G., Patrick, M. L., Xi, W., Matey, V. and Val, A. L. (2010). Impact of ontogenetic changes in branchial morphology on gill function in Arapaima gigas. *Physiol. Biochem. Zool.* **83**, 322-332. doi:10.1086/648568

Graham, J. B. (1997a). Chapter 2 - Diversity and natural history. In *Air-Breathing Fishes* (ed. J. B. Graham), pp. 13-63. San Diego: Academic Press.

Graham, J. B. (1997b). Chapter 3 - Respiratory organs. In *Air-Breathing Fishes* (ed. J. B. Graham), pp. 65-133. San Diego: Academic Press.

Graham, J. B. (1997c). Chapter 5 - Aerial and aquatic gas exchange. In *Air-Breathing Fishes* (ed. J. B. Graham), pp. 153-181. San Diego: Academic Press.

Graham, J. B. (1997d). Chapter 4 - Circulatory adaptations. In *Air-Breathing Fishes* (ed. J. B. Graham), pp. 135-151. San Diego: Academic Press.

Graham, J. B. (1983). The Transition to Air Breathing in Fishes: II. Effects of Hypoxia Acclimation on the Bimodal Gas Exchange of Ancistrus Chagresi (Loricariidae). *J. Exp. Biol.* **102**, 157-173. doi:10.1242/jeb.102.1.157

Graham, J. B. and Wegner, N. C. (2010). Breathing air in water and in air: the air-breathing fishes. In *Respiratory Physiology of Vertebrates: Life With and Without Oxygen* (ed. G. E. Nilsson), pp. 174-221. Cambridge: Cambridge University Press.

Graham, J. B., Kramer, D. L. and Pineda, E. (1978). Comparative respiration of an air-breathing and a non-air-breathing characoid fish and the evolution of aerial respiration in Characins. *Physiol. Zool.* **51**, 279-288. doi:10.1086/physzool.51.3.30155745

Greenwood, P. H. and Liem, K. F. (1984). Aspiratory respiration in Arapaima gigas (Teleostei, Osteoglossomorpha): a reappraisal. *J. Zool.* **203**, 411-425. doi:10.1111/j.1469-7998.1984.tb02341.x

Harter, T. S., Brauner, C. J. and Matthews, P. G. D. (2017). A novel technique for the precise measurement of CO2 production rate in small aquatic organisms as validated on aeshnid dragonfly nymphs. *J. Exp. Biol.* **220**, 964. doi:10.1242/jeb.150235

Hartzler, L. K., Munns, S. L., Bennett, A. F. and Hicks, J. W. (2006). Recovery from an activity-induced metabolic acidosis in the American alligator, Alligator mississippiensis. *Comp. Biochem. Physiol. A Mol. Integr. Physiol.* **143**, 368-374. doi:10.1016/j.cbpa.2005.12.024

Hothorn, T., Bretz, F., Ag, P. and Westfall, P. (2015). Simultaneous inference in general parametric models. *Biom. J.* 50, 346-363. doi:10.1002/bimj.200810425

Hughes, G. M. and Singh, B. N. (1970). Respiration in an air-breathing fish, the climbing perch anabas testudineus bloch: i. oxygen uptake and carbon dioxide release into air and water. *J. Exp. Biol.* **53**, 265-280. doi:10.1242/jeb.53.2.265

Hughes, G. M. and Singh, B. N. (1971). Gas exchange with air and water in an air-breathing catfish, Saccobranchus (≡Heteropneustes) Fossilis. *J. Exp. Biol.* **55**, 667-682. doi:10.1242/jeb.55.3.667

Ishimatsu, A. (2012). Evolution of the cardiorespiratory system in air-breathing fishes. *Aqua-BioScience Monographs* **5**, 1-28. doi:10.5047/absm.2012.00501.0001

Ishimatsu, A. and Itazawa, Y. (1983). Difference in blood oxygen levels in the outflow vessels of the heart of an air-breathing fish,Channa argus: Do separate blood streams exist in a teleostean heart? *J. Comp. Physiol.* **149**, 435-440. doi:10.1007/BF00690000

Iversen, N. K., Lauridsen, H., Huong, D. T. T., Van Cong, N., Gesser, H., Buchanan, R., Bayley, M., Pedersen, M. and Wang, T. (2013). Cardiovascular anatomy and cardiac function in the air-breathing swamp eel (Monopterus albus). *Comp. Biochem. Physiol. A Mol. Integr. Physiol.* **164**, 171-180. doi:10.1016/j.cbpa.2012.08.007

Johansen, K. (1970). 9 Air breathing in fishes. In *Fish Physiology*, Vol. 4 (eds. W. S. Hoar and D. J. Randall), pp. 361-411. Academic Press.

Johansen, K., Lenfant, C. and Hanson, D. (1968). Cardiovascular dynamics in the lungfishes. *Zeitschrift für vergleichende Physiologie* **59**, 157-186. doi:10.1007/BF00339348

Johansen, K., Mangum, C. P. and Weber, R. E. (1978). Reduced blood O2 affinity associated with air breathing in osteoglossid fishes. *Can. J. Zool.* **56**, 891-897. doi:10.1139/z78-124

Keys, A. B. (1930). The measurement of the respiratory exchange of aquatic animals. *Biol. Bull.* **59**, 187-198. doi:10.2307/1536988

Kleiber, M. (1961). *The Fire of Life; An Introduction to Animal Energetics*. New York: Wiley.

Lauff, R. F. and Wood, C. M. (1996). Respiratory gas exchange, nitrogenous waste excretion, and fuel usage during starvation in juvenile rainbow trout, Oncorhynchus mykiss. *J. Comp. Physiol. B* **165**, 542-551. doi:10.1007/BF00387515

Lefevre, S., Huong, D. T. T., Wang, T., Phuong, N. T. and Bayley, M. (2011). Hypoxia tolerance and partitioning of bimodal respiration in the striped catfish (Pangasianodon hypophthalmus). *Comp. Biochem. Physiol. A Mol. Integr. Physiol.* **158**, 207-214. doi:10.1016/j.cbpa.2010.10.029

Lefevre, S., Huong, D. T. T., Phuong, N. T., Wang, T. and Bayley, M. (2012). Effects of hypoxia on the partitioning of oxygen uptake and the rise in metabolism during digestion in the air-breathing fish Channa striata. *Aquaculture* **364-365**, 137-142. doi:10.1016/j.aquaculture.2012.08.019

Lefevre, S., Wang, T., Huong, D. T. T., Phuong, N. T. and Bayley, M. (2013). Partitioning of oxygen uptake and cost of surfacing during swimming in the air-breathing catfish Pangasianodon hypophthalmus. *J. Comp. Physiol. B* **183**, 215-221.

Lefevre, S., Wang, T., Jensen, A., Cong, N. V., Huong, D. T. T., Phuong, N. T. and Bayley, M. (2014). Air-breathing fishes in aquaculture. What can we learn from physiology? *J. Fish Biol.* **84**, 705-731. doi:10.1111/jfb.12302

Lefevre, S., Bayley, M. and McKenzie, D. J. (2016). Measuring oxygen uptake in fishes with bimodal respiration. *J. Fish Biol.* **88**, 206-231. doi:10.1111/jfb.12698

Malte, H. and Weber, R. E. (1985). A mathematical model for gas exchange in the fish gill based on non-linear blood gas equilibrium curves. *Respir. Physiol.* **62**, 359-374. doi:10.1016/0034-5687(85)90091-X

Mandic, M., Pan, Y. K., Gilmour, K. M. and Perry, S. F. (2020). Relationships between the peak hypoxic ventilatory response and critical O2 tension in larval and adult zebrafish (Danio rerio). *J. Exp. Biol.* **223**, jeb213942. doi:10.1242/jeb.213942

Mattias, A. T., Rantin, F. T. and Fernandes, M. N. (1998). Gill respiratory parameters during progressive hypoxia in the facultative air-breathing fish, Hypostomus regani (Loricariidae). *Comp. Biochem. Physiol. A Mol. Integr. Physiol.* **120**, 311-315. doi:10.1016/S1095-6433(98)00034-8

Oliveira, R. D., Lopes, J. M., Sanches, J. R., Kalinin, A. L., Glass, M. L. and Rantin, F. T. (2004). Cardiorespiratory responses of the facultative air-breathing fish jeju, Hoplerythrinus unitaeniatus (Teleostei, Erythrinidae), exposed to graded ambient hypoxia. *Comp. Biochem. Physiol. A Mol. Integr. Physiol.* **139**, 479-485. doi:10.1016/j.cbpb.2004.10.011

Olson, K. R. (1994). Circulatory anatomy in bimodally breathing fish. *Am. Zool.* **34**, 280-288. doi:10.1093/icb/34.2.280

Pelster, B., Wood, C. M., Braz-Mota, S. and Val, A. L. (2020). Gills and air-breathing organ in O2 uptake, CO2 excretion, N-waste excretion, and ionoregulation in small and large pirarucu (Arapaima gigas). *J. Comp. Physiol. B* **190**, 569-583. doi:10.1007/s00360-020-01286-1

Perry, S. F. and Gilmour, K. M. (2002). Sensing and transfer of respiratory gases at the fish gill. *J. Exp. Zool.* **293**, 249-263. doi:10.1002/jez.10129

Perry, S. F., Jonz, M. G. and Gilmour, K. M. (2009). Chapter 5 oxygen sensing and the hypoxic ventilatory response. In *Fish Physiology*, Vol. 27 (ed. J. G. Richards, A. P. Farrell and C. J. Brauner), pp. 193-253. Academic Press.

Phuong, L. M., Huong, D. T. T., Nyengaard, J. R. and Bayley, M. (2017). Gill remodelling and growth rate of striped catfish Pangasianodon hypophthalmus under impacts of hypoxia and temperature. *Comp. Biochem. Physiol. A Mol. Integr. Physiol.* **203**, 288-296. doi:10.1016/j.cbpa.2016.10.006

Phuong, L. M., Huong, D. T. T., Malte, H., Nyengaard, J. R. and Bayley, M. (2018). Ontogeny and morphometrics of the gills and swim bladder of air-breathing striped catfish Pangasianodon hypophthalmus. *J. Exp. Biol.* **221**, jeb168658. doi:10.1242/jeb.168658

Rahmatullah, M. and Boyde, T. R. C. (1980). Improvements in the determination of urea using diacetyl monoxime; methods with and without deproteinisation. *Clin. Chim. Acta* **107**, 3-9. doi:10.1016/0009-8981(80)90407-6

Rahn, H. and Howell, B. J. (1976). Bimodal gas exchange. In *Respiration of Amphibious Vertebrates* (ed. G. M. Hughes), pp. 271-285. Academic Press.

Ramírez, C., Coronado, J., Silva, A. and Romero, J. (2018). Cetobacterium is a major component of the microbiome of giant Amazonian Fish (Arapaima gigas) in Ecuador. *Animals* **8**. doi:10.3390/ani8110189

Randall, D. J., Farrell, A. P. and Haswell, M. S. (1978). Carbon dioxide excretion in the pirarucu (Arapaima gigas), an obligate air-breathing fish. *Can. J. Zool.* **56**, 977-982. doi:10.1139/z78-136

Randall, D. J., Cameron, J. N., Daxboeck, C. and Smatresk, N. (1981a). Aspects of bimodal gas exchange in the bowfin, Amia calva L. (actinopterygii: amiiformes). *Respir. Physiol.* **43**, 339-348. doi:10.1016/0034-5687(81)90114-6

Randall, D., Burggren, W., Farrell, A. and Haswell, M. (1981b). Ventilation and perfusion relationships. In *The Evolution of Air Breathing in Vertebrates* (eds. A. P. Farrell, D. J. Randall, M. S. Haswell and W. W. Burggren), pp. 52-76. Cambridge: Cambridge University Press.

Richards, J. G., Wang, Y. S., Brauner, C. J., Gonzalez, R. J., Patrick, M. L., Schulte, P. M., Choppari-Gomes, A. R., Almeida-Val, V. M. and Val, A. L. (2007). Metabolic and ionoregulatory responses of the Amazonian cichlid, Astronotus ocellatus, to severe hypoxia. *J. Comp. Physiol. B* **177**, 361-374. doi:10.1007/s00360-006-0135-2

Robergs, R. A., Ghiasvand, F. and Parker, D. (2004). Biochemistry of exercise-induced metabolic acidosis. *Am. J. Physiol. Regul. Integr. Comp. Physiol.* **287**, R502-R516. doi:10.1152/ajpregu.00114.2004

Scadeng, M., McKenzie, C., He, W., Bartsch, H., Dubowitz, D. J., Stec, D. and St, and Leger, J. (2020). Morphology of the amazonian teleost genus arapaima using advanced 3D imaging. *Front. Physiol.* **11**. doi:10.3389/fphys.2020.00260

Scott, G. R., Matey, V., Mendoza, J.-A., Gilmour, K. M., Perry, S. F., Almeida-Val, V. M. F. and Val, A. L. (2017). Air breathing and aquatic gas exchange during hypoxia in armoured catfish. *J. Comp. Physiol. B* **187**, 117-133. doi:10.1007/s00360-016-1024-y

Singh, B. (1976). Balance between aquatic and aerial respiration. *Respir. Amphibious Vertebr.* **33**, 125-164. doi:10.1159/000193730

Smatresk, N. J. (1990). Chemoreceptor modulation of endogenous respiratory rhythms in vertebrates. *Am. J. Physiol.* **259**, R887-R897. doi:10.1152/ajpregu.1990.259.5.R887

Smatresk, N. J. and Cameron, J. N. (1982). Respiration and Acid-Base Physiology of the Spotted Gar, A Bimodal Breather: I. Normal Values, and the Response to Severe Hypoxia. *J. Exp. Biol.* **96**, 263-280. doi:10.1242/jeb.96.1.263

Stevens, E. D. and Holeton, G. F. (1978). The partitioning of oxygen uptake from air and from water by the large obligate air-breathing teleost pirarucu (Arapaima gigas). *Can. J. Zool.* **56**, 974-976. doi:10.1139/z78-135

Thomsen, M. T., Wang, T., Milsom, W. K. and Bayley, M. (2017). Lactate provides a strong pH-independent ventilatory signal in the facultative air-breathing teleost Pangasianodon hypophthalmus. *Sci. Rep.* **7**, 6378. doi:10.1038/s41598-017-06745-4

Thomsen, M. T., Lefevre, S., Nilsson, G. E., Wang, T. and Bayley, M. (2019). Effects of lactate ions on the cardiorespiratory system in rainbow trout (Oncorhynchus mykiss). *Am. J. Physiol. Regul. Integr. Comp. Physiol.* **316**, R607-R620. doi:10.1152/ajpregu.00395.2018

Tzaneva, V., Vadeboncoeur, C., Ting, J. and Perry, S. F. (2014). Effects of hypoxia-induced gill remodelling on the innervation and distribution of ionocytes in the gill of goldfish, Carassius auratus. *J. Comp. Neurol.* **522**, 118-130. doi:10.1002/cne.23392

Verdouw, H., Van Echteld, C. J. A. and Dekkers, E. M. J. (1978). Ammonia determination based on indophenol formation with sodium salicylate. *Water Res.* **12**, 399-402. doi:10.1016/0043-1354(78)90107-0

Wang, S., Carter, C. G., Fitzgibbon, Q. P. and Smith, G. G. (2021). Respiratory quotient and the stoichiometric approach to investigating metabolic energy substrate use in aquatic ectotherms. *Rev. Aquacult.* **13**, 1255-1284. doi:10.1111/raq.12522

Wood, C. M., Pelster, B., Braz-Mota, S. and Val, A. L. (2020). Gills versus kidney for ionoregulation in the obligate air-breathing Arapaima gigas, a fish with a kidney in its air-breathing organ. *J. Exp. Biol.* **223**, jeb232694. doi:10.1242/jeb.232694

Yu, K. L. and Woo, N. Y. S. (1985). Effects of ambient oxygen tension and temperature on the bimodal respiration of an air-breathing teleost, Channa maculata. *Physiol. Zool.* **58**, 181-189. doi:10.1086/physzool.58.2.30158565

Fig. S1. Accuracy and repeatability of the artificial lung

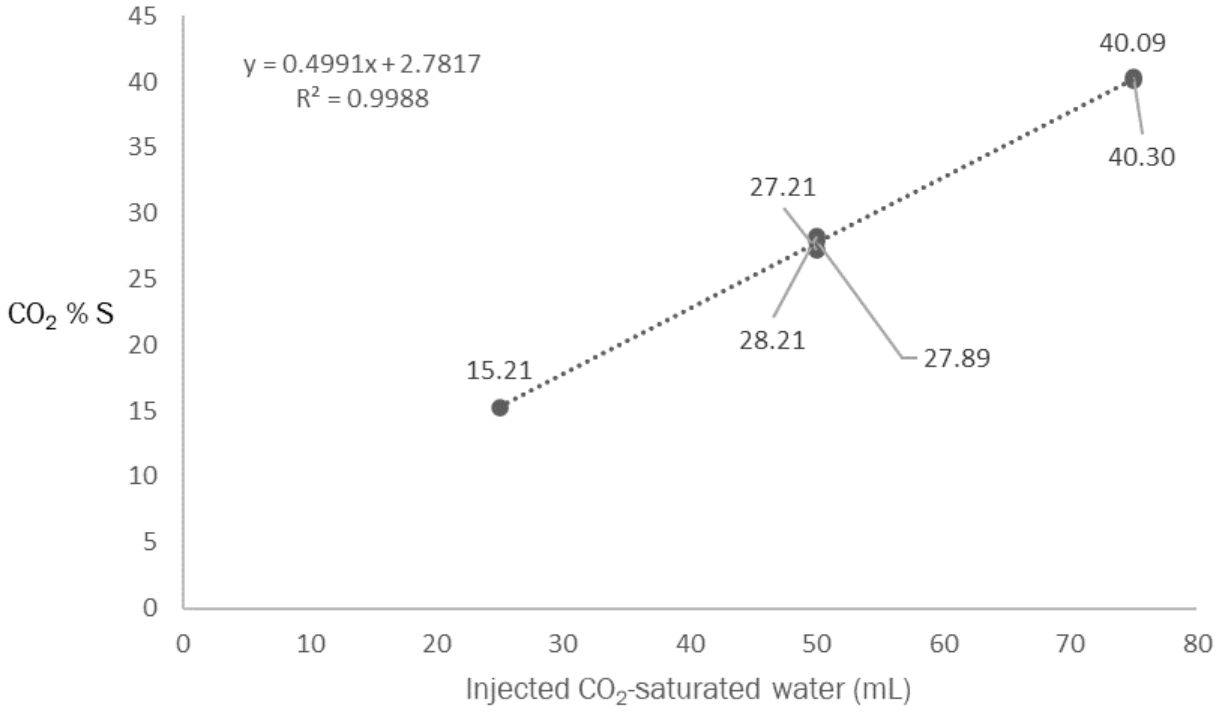

Six CO_2-saturated water injections were made and measured in the order 50, 50, 25, 75, 75 and 50 ml.

Fig. S1 shows a pilot calibration test where eight injections where measured based on three different volumes of CO_2 injected (25 ml, 50 ml, and 75 ml (755, 1510 and 2265 µmol CO_2)), based on the method described in the CO_2 water measurement section (**2.3.3**). This validation of the apparatus shows the accurate repeatability and linearity of the system. A linear slope indicates that the calibration factor does not differ when different CO_2 concentrations are measured, which means that a single injection after each replicate is enough to accurately calibrate the system even when the fish varies in amount of CO_2 excreted during the measurement (e.g., high stress values vs low relaxed values). The accurate repeatability of the system is indicated by the overlapping measurements. The chamber had been flushed twice before injections to equilibrate the system.

Fig. S2. Ammonia and Urea baseline increase

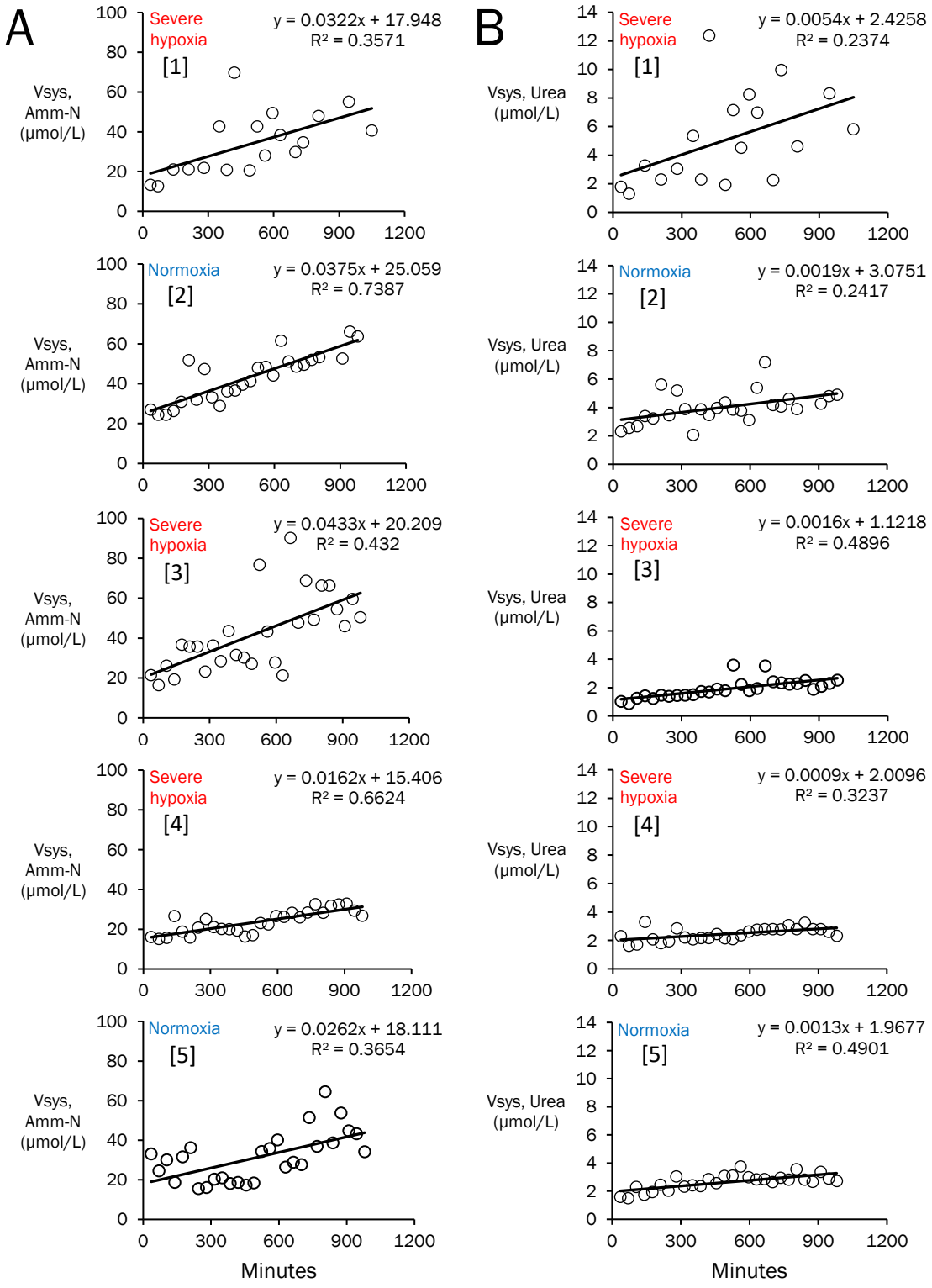

Journal of Experimental Biology • Supplementary information

These plots show the concentration increase of total Ammonia-N (A) and Urea-N (B) in the whole system water volume (~240 L) for Arapaima gigas (n=5). Water treatment is shown by 'Normoxia' and 'Severe hypoxia'. Individual experiments are displayed with unique bracketed [ ] numbers.

We could not reliably measure the elevations of the concentrations of the N-wastes inside the chamber during each closed period. We instead considered the water samples made at the beginning of each closed period (note: just after flushing the chamber with header-tank water) as being a sample from the entire system's water volume (chamber + header-tank). Thus, we calculated an average excretion rate for the entire measurement period (~17.5h) by performing a linear regression on the system's concentration increase of both ammonia-N and urea-N (Fig. S2).